Cross-linkable Microgel Composite Matrix Bath for Embedded Bioprinting of Perfusable Tissue Constructs and Sculpting of Solid Objects

Ashley M. Compaan[1,*], Kaidong Song[2], Wenxuan Chai[2], Yong Huang[1, 2, 3,$]

[1]Department of Materials Science and Engineering, University of Florida, Gainesville, FL 32611, USA.

[2]Department of Mechanical and Aerospace Engineering, University of Florida, Gainesville, FL 32611, USA.

[3]Department of Biomedical Engineering, University of Florida, Gainesville, FL 32611, USA.

*Novabone Products, LLC. 13510 NW US Highway 441, Alachua, FL, 32615 USA.

[$]Corresponding author

Keywords: cross-linkable matrix bath, microgel composite matrix, embedded bioprinting, perfusable tissue construct, solid object sculpting

<u>Abstract</u>

Tissue engineering is a rapidly growing field which requires advanced fabrication technologies to generate cell-laden tissue analogs with a wide range of internal and external physical features including perfusable channels, cavities, custom shapes, and spatially varying material and/or cell compositions. A versatile embedded printing methodology is proposed in this work for creating custom biomedical acellular and cell-laden hydrogel constructs by utilizing a biocompatible microgel composite matrix bath. Sacrificial material is patterned within a biocompatible

hydrogel precursor matrix bath using extrusion printing to create three-dimensional (3D) features; after printing, the matrix bath is cross-linked, and the sacrificial material is flushed away to create perfusable channels within the bulk composite hydrogel matrix. The composite matrix bath material consists of jammed cross-linked hydrogel microparticles (microgels) to control rheology during fabrication along with a fluid hydrogel precursor which is cross-linked after fabrication to form the continuous phase of the composite hydrogel. For demonstration, gellan or enzymatically cross-linked gelatin microgels are utilized with a continuous gelatin hydrogel precursor solution to make the composite matrix bath herein; the composite hydrogel matrix is formed by cross-linking the continuous gelatin phase enzymatically after printing. A variety of features including discrete channels, junctions, networks, and external contours are fabricated in the proposed composite matrix bath using embedded printing. Cell-laden constructs with printed features are also evaluated; the microgel composite hydrogel matrices support cell activity, and printed channels enhance proliferation compared to solid constructs even in static culture. The proposed method can be expanded as a solid object sculpting method to sculpt external contours by printing a shell of sacrificial ink and further discarding excess composite hydrogel matrix after printing and cross-linking. While aqueous alginate solution is used as a sacrificial ink, more advanced sacrificial materials can be utilized for better printing resolution.

1. Introduction

The progress of tissue engineering has been recently promoted by three-dimensional (3D) printing.[1-8] For tissue engineering to be clinically relevant, the capability to fabricate perfusable thick tissues is indispensable. Herein, thick tissues are referred to cellular tissues with a thickness higher than the diffusion limit (usually 200 μm or less approximately). Fortunately, 3D printing

can be utilized to fabricate perfusable thick tissues in two complementary ways: freeform fabrication in which the build material forms a final construct or printing a sacrificial template to define perfusable features within a cast construct. Various approaches to print living cell-laden tubular structures or perfusable channels by freeform fabrication have been developed including inkjetting,[9,10] laser printing,[11] and bath-supported extrusion.[12-17] However, directly printing a perfusable thick construct, while having fewer steps than approaches using sacrificial materials, is inefficient because the bulk ink material occupies most of the construct volume; furthermore, the channel morphology may not be smooth enough even if perfusable thick constructs are achievable.

Alternatively, 3D printed templates made of a sacrificial material have been more extensively investigated for generating channel networks within biological constructs[18-27] to mimic vascularized thick tissues. There are two basic implementations of this strategy: casting a matrix material around a pre-printed sacrificial template (printing-then-casting) or printing a sacrificial template within a matrix precursor in the mold cavity (casting-then-printing, or embedded printing). In general, after the sacrificial template is embedded in a matrix precursor material, the matrix is cured and the sacrificial material is liquefied to create voids in the desired configuration within the construct. The printing-then-casting process is compatible with various sacrificial and matrix materials, relatively simple to implement, and requires no specific material characteristics, save that the sacrificial material be soluble in some condition where the matrix is stable. However, this approach is limited to simple 3D self-supporting sacrificial templates. Complicated 3D self-supporting templates are difficult to print for many applications, and sacrificial templates are easily damaged during matrix casting.

In the casting-then-printing/embedded printing approach, sacrificial material is patterned within the matrix precursor, a concept which has been successfully demonstrated in acellular and cellular applications.[28-33] This allows simultaneous control of the template architecture and placement within the overall construct while minimizing handling since the construct is formed in a single step and can be formed within a fixture. While attractive, this casting-then-printing approach requires that the matrix have special rheological properties in order to retain the desired arrangement of sacrificial materials. In general, optimal matrix materials should be yield stress materials for embedded printing and cross-linkable to form bulk solids or gels after the embedded pattern is complete. Yield stress materials are structured or complex fluids which behave as elastic solids at rest but transition to liquid-like, often shear thinning, behavior upon an applied shear stress; such as material-specific threshold shear stress is designated the yield stress. This type of rheological behavior is a result of micro- and/or nano-scale structural units or features within the fluid which must be rearranged for flow to take place. Unfortunately, single hydrogel matrix materials which are intrinsically suited to this embedded printing process are rare. To date, only pluronic-based hydrogels[25] and specially designed guest-host hydrogels[30] have been reported. However, pluronics are generally unsuitable for cell culture[34] and guest-host hydrogels may lack long-term stability.[30]

This study aims to design a cytocompatible hydrogel precursor composite such that it retains the yield stress properties of the jammed microgel filler material to enable stable embedded pattern formation within a continuous curable matrix bath material. Specifically, biocompatible microgel particles are utilized as fillers in a continuous cross-linkable hydrogel precursor phase to prepare composite matrix bath materials suitable for embedded printing. Thus, the entire construct matrix

can be stabilized after fabrication for subsequent removal of the sacrificial ink and maturation of engineered tissues.

In contrast to prior 3D bioprinting work using similar materials,[17] the matrix bath material forms the final construct while the printed ink serves as a temporary sacrificial patterning agent. While prior work explored the use of gellan microgels as a sacrificial support bath material, this study utilizes them as part of the final composite matrix bath, essentially inverting the printing process in order to efficiently fabricate bulky perfusable cross-linked cell-laden hydrogel constructs. This design approach has additional benefits. Composite materials offer more tunable mechanical and chemical properties to better mimic tissue properties since both filler and continuous phase can be adjusted. Other features may be added to either component as well: encapsulated soluble factors to direct cell behavior[35] and chemical functionalities to enable controlled or cell-mediated degradation[35] are just a couple of the possibilities. Yield stress materials also prevent particle (cell) sedimentation[36], enabling consistent cell distribution throughout the construct even if the gel formation process is slow. Finally, cells and continuous matrix material form an interconnected network around filler particles,[37,38] which increases the effective local cell density and promotes cellular interactions. Similar microgel-reinforced hydrogels have been found to be superior to either the pure matrix material or a double network comprised of the two polymers for engineered tissue applications; [35,39] fabrication is more convenient, properties easier to adjust, and cells are more functional in the microgel composites. If the filler is degradable, the maturing tissue can eventually fill the voids left behind; [35] if it is simply inert and biocompatible, then it provides extra volume to the tissue construct without consuming additional nutrients or producing waste, which may be advantageous in clinical soft tissue repair. The microgel

composite matrix bath-based embedded printing approach therefore simultaneously addresses two major concerns[40] in tissue engineering: achieving physiological cell density and perfusing engineered constructs. The matrix bath material design intrinsically elevates the local cell density by a factor of approximately 10, assuming that the microgels occupy 90% of the construct volume. In addition, the ability to print channels within bulk constructs enables fabrication of large-scale perfusable tissue analogues using readily available materials and equipment.

2. Cross-linkable Microgel Composite Matrix Bath for Embedded Printing

2.1 Concept of embedded printing

The printing process for embedded printing is illustrated in **Figure 1**. First, a reservoir is filled with the solid-like matrix bath material at rest. For this work, the composite matrix bath consists of jammed microgels (gellan or gelatin-based) as the filler to adjust rheology and hydrogel precursor (gelatin-based) as the continuous matrix (Figure 1(a)). Sacrificial material is deposited from a moving extrusion tip in the uncured matrix bath material to create features within the printing reservoir (Figure 1(b)). The bulk matrix bath material liquefies upon the shear stress from the moving extrusion tip as the microgels slide past each other (Figure 1(b) inset) to be liquefied to allow sacrificial ink to be deposited. Then the microgels turn to a jammed solid-like state to trap the deposited sacrificial material (Figure 1(c)). After the gelation process is complete (Figure 1(d)), the sacrificial material is removed to create void space or channels surrounded by the cross-linked composite hydrogel matrix as illustrated in Figure 1(e).
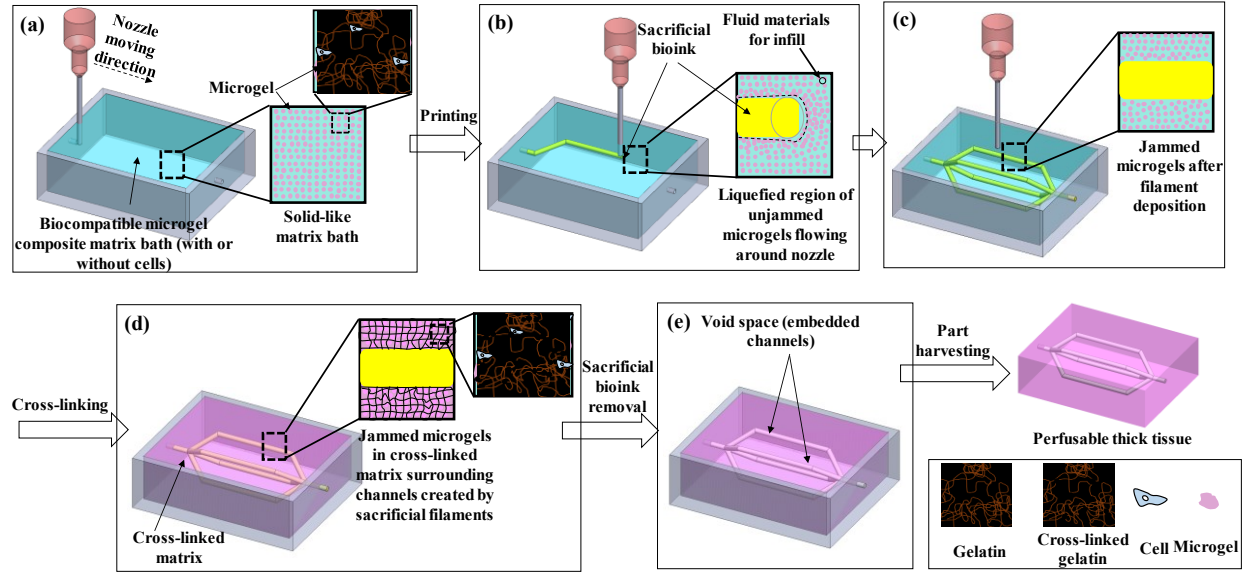
Figure 1. Printing schematic showing local behavior of the (a) static and (b) disrupted matrix bath material during printing as well as (c) stabilization of deposited sacrificial fluid by solid-like composite hydrogel matrix after printing. After (d) cross-linking, it shows (e) final construct macrostructural and microstructural features.

2.2 Microgel composite matrix bath design

The microgel-based composite matrix bath formulations, which are made of microgel filler particles in a continuous cross-linkable hydrogel precursor phase, are designed to have appropriate rheological properties, biocompatibility, working time, and mechanical properties. Two microgel materials are explored herein: gellan and gelatin. The microgel particles are formed as a dispersion from fragmented hydrogels, and they have a yield stress as jammed systems. For the continuous phase of composite matrix bath material formulations, unmodified gelatin is utilized in this work; the continuous phase is cross-linked using transglutaminase (TG) to form stable constructs after printing is complete. **Figure 2** illustrates the nature of the gelatin

7

continuous phase and microgel particles (Figure 2(a)), and shows essential aspects of the gelatin-

gellan matrix bath (Figure 2(b-g)) and gelatin-gelatin matrix bath (Figure 2(h-k)) formulations.
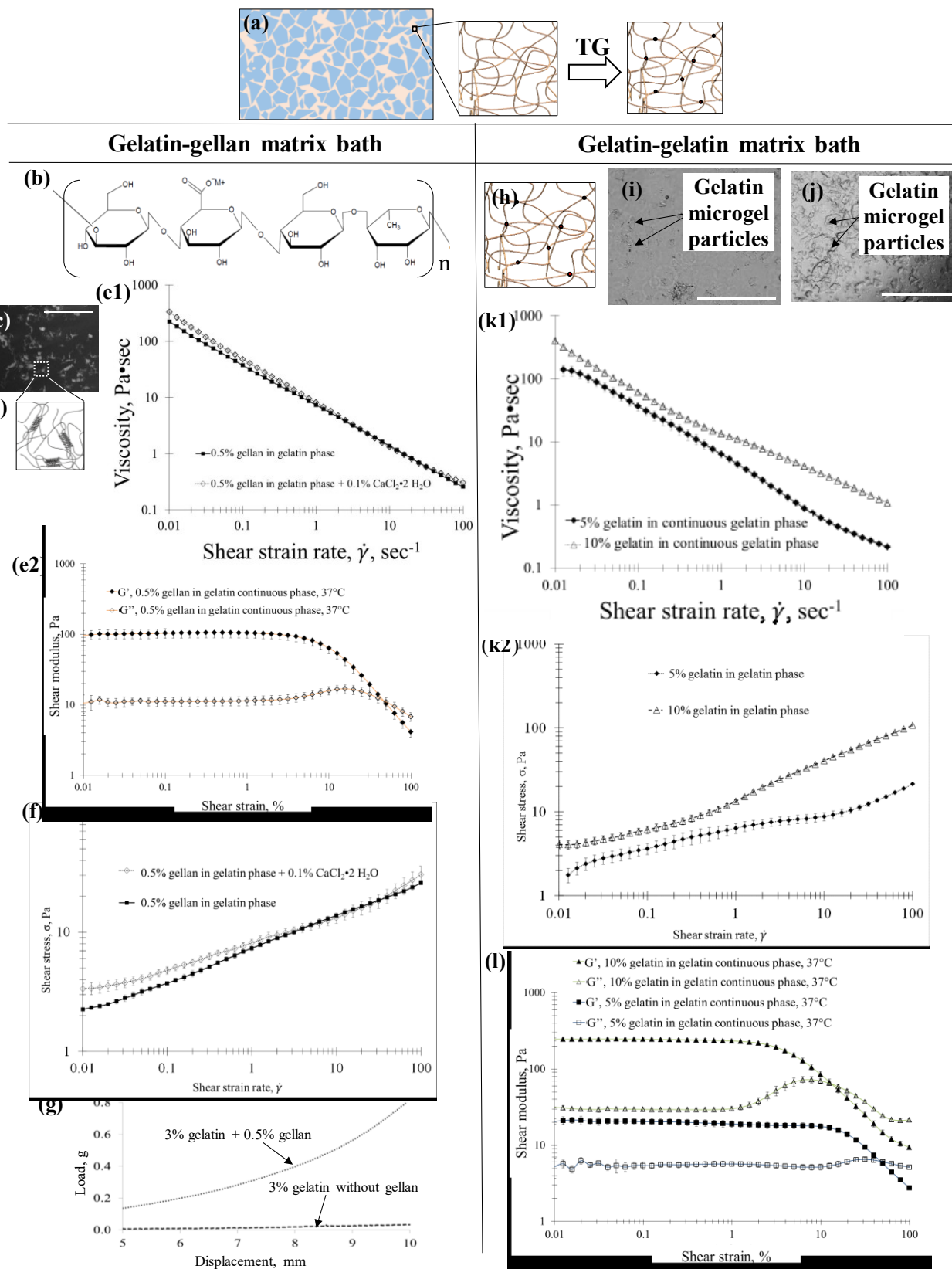
(a) TG

Gelatin-gellan matrix bath

(b)

(e1)

Viscosity, Pa·sec

- —0.5% gellan in gelatin phase
- —0.5% gellan in gelatin phase + 0.1% CaCl$_2$·2 H$_2$O

Shear strain rate, $\dot{\gamma}$, sec^{-1}

(c)

(d)

(e2)

- ◆ G', 0.5% gellan in gelatin continuous phase, 37°C
- ◇ G'', 0.5% gellan in gelatin continuous phase, 37°C

Shear modulus, Pa

Shear strain, %

(f)

- ○ 0.5% gellan in gelatin phase + 0.1% CaCl$_2$·2 H$_2$O
- ■ 0.5% gellan in gelatin phase

Shear stress, σ, Pa

Shear strain rate, $\dot{\gamma}$

(g)

Load, g

3% gelatin + 0.5% gellan

3% gelatin without gellan

Displacement, mm

Gelatin-gelatin matrix bath

(h)

(i) Gelatin microgel particles

(j) Gelatin microgel particles

(k1)

Viscosity, Pa•sec

- ◆ 5% gelatin in continuous gelatin phase
- △ 10% gelatin in continuous gelatin phase

Shear strain rate, $\dot{\gamma}$, sec^{-1}

(k2)

- ◆ 5% gelatin in gelatin phase
- △ 10% gelatin in gelatin phase

Shear stress, σ, Pa

Shear strain rate, $\dot{\gamma}$

(l)

- ▲ G', 10% gelatin in gelatin continuous phase, 37°C
- △ G'', 10% gelatin in gelatin continuous phase, 37°C
- ■ G', 5% gelatin in gelatin continuous phase, 37°C
- □ G'', 5% gelatin in gelatin continuous phase, 37°C

Shear modulus, Pa

Shear strain, %

9

Figure 2. Representative microgel composite matrix bath properties. (a) schematic of matrix showing microgel particles (blue) in continuous gelatin matrix (beige); inset: schematic of gelatin in solution and after cross-linking with TG, (b) chemical structure of gellan, (c) gellan microgel particles, (d) schematic of gellan gelation by aggregation of helices, (e1-f) rheology of gelatin-gellan composite matrix bath to quantify the yield stress behavior at 37°C, (g) mechanical behavior of gelatin (without gellan) and gelatin-gellan microgel composite, (h) schematic of covalently cross-linked gelatin microgel, (i-j) optical micrographs of 5% and 10% gelatin microgels, and (k1-l) rheology of gelatin-gelatin composite matrix bath at 37°C. (Scale bars: 1 mm)

2.2.1 Gellan microgels

As a linear anionic microbial polysaccharide, gellan has been widely used in tissue engineering, drug delivery, and food science.[41,42] Its repeat unit is a tetrasaccharide sequence (Figure 2(a)), and the widely used low acyl version of gellan is utilized herein. Once heated, gellan molecules have a random coil configuration in aqueous solution; upon cooling, some regions come to be helical and aggregate to form a bulk hydrogel as physical cross-linking (Figure 2(b)). Hydrogels formed by low acyl gellan are clear, brittle and can be further made as microgels. [43] Gellan hydrogels formed in the presence of monovalent salts are thermoreversible, while divalent salts significantly increase thermal stability and make the gels essentially irreversible. For this work, gellan was prepared at 0.5% w/v in phosphate buffered saline (PBS) according to preliminary results.[17] Stainless steel mesh was used to fragment bulk gellan gels, resulting in a dispersion of irregular particles and particle aggregates (average diameter 50 ± 34 µm based on light scattering data, and average aspect ratio 1.6 based on microscopic image analysis (Figure 2(c)). The gellan

concentration was fixed at 0.5% since this composition provides suitable yield stress and shear thinning rheology to the matrix bath formulations for the printing process, as shown in Figure 2(e1) and (e2). In addition, oscillatory strain sweep data (Figure 2(f)) confirms that the gelatin-gellan matrix bath material transitions from solid-like behavior, as indicated by a larger storage modulus, to fluid-like behavior, indicated by a larger loss modulus, at around 50% strain. This shear-induced liquefaction is localized to the volume immediately around the traveling tip since the matrix bath liquefies at considerably less than 100% strain.

2.2.2 Gelatin microgels

To demonstrate the versatility of this approach, gelatin microgels are also utilized. Derived from collagen, gelatin is widely used for biomedical applications. It may transform from a physical hydrogel to be liquefied at approximately 35°C. For physiological stability, gelatin can be cross-linked chemically using a variety of cross-linking agents; recent work has identified the enzyme TG as an optimal cross-linking agent for biomedical applications for *in vitro* and *in vivo* applications.[44] TG is an enzyme which covalently links gelatin molecules to one another, forming a cross-linked network. Of different enzymes, transglutaminases (TGs) help cross-link protein molecules covalently and have been utilized to gel protein-based hydrogels including gelatin and collagen [21,45,46] and result in physiologically stable constructs. As such, TG is utilized in this work. Many other strategies for forming physiologically stable gelatin hydrogels such as gelatin methacrylate (GelMA) have been developed, but they generally require chemical modification of native gelatin to introduce the functional groups necessary for controlled physical or chemical hydrogel formation. Also, the stimuli such as ultraviolet irradiation needed to cross-link the modified gelatin might injure living cells. [47-49] For these reasons, native gelatin

is used in this work to bypass the complicated process for preparing modified gelatin materials and avoid possible damage during gelation. Additionally, the gelatin gelation time depends on the enzyme concentration, but the final gel properties do not change since the enzyme continues to create cross-links until no more active sites are available. Enzymatic cross-linking can be terminated by heat inactivation of the enzyme above 70°C [50] at some defined time point to produce cross-linked gels with intermediate properties. Covalently cross-linked gelatin, like gellan, can be processed to form jammed microgel dispersions which are yield stress fluids.

In this work, two gelatin concentrations, 5% and 10% w/v in PBS, were utilized to prepare microgels from bulk gels cross-linked using 0.5% and 1% TG, respectively, for 4 hr at 37°C. Both concentrations were chosen in order to have desirable mechanical stiffness of printed constructs for good structural integrity as well as good cell proliferation. Similar particle size distributions (260 ± 200 μm particle dimensions for 10% gelatin and 125 ± 100 μm particles for 5% gelatin based on light scattering data) and morphologies are observed for both gelatin concentrations. Compared to gellan, the gelatin particles appear to be rougher with generally lower aspect ratios (average aspect ratio 1.4 for both gelatin concentrations while 1.6 for gellan based on image analysis). This is attributed to the tearing and agitation during the blending process to produce gelatin microgels as well as the higher elasticity of the gelatin bulk gels which causes them to tear rather than shatter during fragmentation. Both gelatin concentrations provide suitable yield stress and shear thinning rheology to the matrix bath formulations for the printing process, as shown in Figure 2(k1) and (k2). In addition, oscillatory strain sweep data (Figure 2(l)) confirms that the gelatin-gelatin matrix bath materials transition from solid-like behavior, as indicated by the fact that the storage modulus is greater than the loss modulus, to

fluid-like behavior, indicated by a larger loss modulus, at less than 50% strain (around 45% for the 5% gelatin microgel formulation, 13% for the 10% gelatin microgel formulation). This shear-induced liquefaction is localized to the volume immediately around the traveling tip since the matrix bath liquefies at considerably less than 100% strain.

2.2.3 Gelatin-based continuous phase

Soluble gelatin which can be cross-linked using TG is employed as the continuous phase of the composite matrix bath material. It is compatible with both gellan and gelatin microgels, provided that the TG within the gelatin microgels is deactivated prior to mixing. If gelatin microgels containing residual active TG are utilized, the mixture begins to gel immediately; it is usable but less convenient. As noted above, the gelation time can be altered by changing the enzyme concentration without strongly affecting the final gel properties since the enzyme continues to create cross-links until no more active sites are available. With a long gelation time, printing can be completed after mixing the matrix with the enzyme, allowing formation of a homogeneously cross-linked construct. However, culture media components may deactivate TG, [51] so for cell-laden constructs the cross-linking process may terminate when they are immersed in or perfused with media. As a result, the mechanical and chemical properties of cell-laden constructs may be more sensitive to the specific fabrication process and matrix bath formulation than acellular structures in which enzymatic cross-linking consumes all possible active sites over time. Combinations of gellan and gelatin have been reported for various biomedical[39,52] and commercial[53] applications. Both of these biopolymers participate in hydrogen bonding and dipole-dipole interactions; positively charged amino acids in gelatin may also interact ionically with the negatively charged carboxylate functional groups in gellan. This results in a strong

interphase between matrix and filler and a structurally sound composite after gelation. Since the gellan is in the form of pre-gelled microgels, the microstructure is fixed and does not evolve over time, as it might if both gellan and gelatin were in solution simultaneously. The reported tendency of fluid gelatin-gellan mixtures to phase separate under physiological conditions[54] implies that the dissolved gelatin remains localized in the space between gellan microgels rather than infiltrating them since gellan-gellan and gelatin-gelatin interactions are favored over gelatin-gellan interactions.

This is the first report using pre-processed gelatin microgel particles as a rheology modifier for producing bulk gelatin constructs. The yield stress behavior imparted by gelatin microgels is similar to that imparted by gellan microgels, but the final composite material has some differences. Because the gelatin particle cross-linking process is terminated by heat inactivation rather than by allowing all active sites to be consumed, the gelatin microgels may participate in covalent cross-links with the surrounding matrix as well as develop additional internal cross-links. Thus, the interphase is exceptionally strong since it consists of both covalent bonds and non-covalent intermolecular interactions. Because both gelatin-gelatin continuous phase and filler are comprised of gelatin, which is chemically similar to native ECM and susceptible to the proteases and other factors which cells secrete to remodel their surroundings, the entire composite volume supports cell adhesion, cell-mediated local degradation, and cell migration.

The combination of gelatin with microgels enables mechanically stable constructs with very low total polymer concentrations (3.5% -13% w/v), which is beneficial since the polymer chains inhibit diffusion through the hydrogel overall; a high polymer concentration makes it more

difficult to supply nutrients and remove waste from cells throughout the bulk construct. Gellan forms robust hydrogels at extremely low concentrations compared to other biopolymers and is therefore uniquely suitable as the microgel component of the composite matrix material for bulk tissue engineering applications. Gelatin microgels are better suited for applications requiring a matrix completely susceptible to cell-mediated degradation.

2.3 Cross-linking of composite matrix bath

Cross-linking of the composite matrix bath material is initiated by the addition of TG immediately before the printing process. After gently mixing to ensure homogeneous gelation, sacrificial material is patterned in the matrix bath material using a 3D extrusion printing system. To maximize working time and explore fabrication of soft materials, the minimum gelatin concentration which would form a stable gel with TG was utilized; based on preliminary work, this nominal concentration was 3%w/v (though the effective concentration is likely higher since pre-gelled microgels exclude gelatin from some fraction of the total volume of the composite). The TG concentration is utilized to control gelation time, primarily, although it also affects the final mechanical properties[55] of the composite since addition of serum-containing culture media inactivates TG. 0.5% TG is found to produce stable, soft gelatin-gellan composite gels in a reasonable amount of time (~75 min) at 37°C while allowing a reasonable printing window using a 37°C heated stage (~35 min). Lowering TG concentration (0.25%) extends the printing window to over 1 hr, but requires an additional 2 hr to form a stable gel; this extended processing time is not ideal for cell laden structures. On the other hand, 1% TG shortens the printing window significantly, making it difficult to complete the printing process before gel formation causes the performance to deteriorate. For gelatin-5% gelatin microgel composites, 0.5% TG

results in much faster cross-linking and a short printing window (~10 min); 0.25% only extends the printing window to ~20 min. This faster gelation is attributed to the availability of cross-linking sites in both the microgel filler and the continuous matrix, resulting in faster development of a covalent network through the whole volume. 0.1% TG results in an adequate printing window with suitable gelation speed using 5% gelatin microgels. For 10% gelatin microgels, the printing window for a given overall TG concentration is slightly longer, which may be due to the higher TG concentration in the microgel formation process which may leave fewer cross-linking sites available within the microgels. As an alternative to the process described herein, a TG-free matrix with TG-supplemented ink was attempted; this strategy is appealing since it limits matrix curing to the patterned region and should conceptually extend the printing window (though perhaps at the expense of consistent gel formation through the entire reservoir). However, this did not produce acceptable results; little or no gel formation was observed.

2.4 Sacrificial ink design

The only requirement for the sacrificial ink in this work is that it has suitable rheology for well-controlled printing by extrusion and is easy to remove after printing. Aqueous 2% alginate in a physiological buffer (PBS) was selected for this work since it is non-toxic and readily available. It is noted that long term exposure to sodium citrate, which is required to liquefy cross-linked alginate templates, might injure encapsulated cells[56,57]. For this reason, uncross-linked alginate is preferred to make sacrificial templates for biomedical applications. While aqueous uncross-linked alginate solution is used as a sacrificial ink for this study, more advanced sacrificial materials should be utilized for better printing resolution in future studies.

3 Material Characterization

2.3.1 Rheological properties

The yield stress behavior of uncross-linked matrix bath formulations is quantified at 37°C, including gelatin-gellan formulations with and without the addition of $CaCl_2$ and gelatin-gelatin formulations as shown in Figure 2(e1), (e2), (k1) and (k2). Steady shear strain rate sweep data are presented using the Herschel-Bulkley model, $\sigma = \sigma_0 + K\dot{\gamma}^n$, where σ is the total stress, σ_0 is the yield stress, $\dot{\gamma}$ is the shear rate, and K and n are fitting parameters; fitting parameters for all formulations are listed in Table 1. For gelatin-gellan, the addition of $CaCl_2$ results in a notable increase in the yield stress, from 0.265 Pa without calcium to 1.78 Pa with added calcium. Similarly, the 5% gelatin microgel formulation has a yield stress of 0.5 Pa while the 10% gelatin microgel formulation has a yield stress of 3.0 Pa. The yield stress of the matrix formulations reported herein are within the range reported in literature for 3D printing applications (0.16 Pa to 8.8 Pa[14]). The low yield stress results in very rapid and complete recovery of the matrix behind the traveling tip so that printed sacrificial material can be trapped effectively. Addition of calcium stiffens the gellan gel particles and therefore causes an increase in the yield stress[58] since additional force is required to deform or compress the microgels to initiate flow. For the same reason, the yield stress of the gelatin-5% gelatin matrix bath material is notably lower than gelatin-10% gelatin matrix bath material since the 10% gelatin microgels are stiffer than 5% gelatin microgels. All of the formulations show strong shear thinning behavior after solid-liquid transitioning under shear, as shown in the insets of Figure 2(e1), (e2), (k1) and (k2) and indicated by the fact that all n values in the Herschel-Bulkley model fits are much smaller than 1.

Table 1. Herschel-Bulkley fitting parameters

Matrix bath formulation	Yield stress, σ_0, Pa	K	n
Gelatin-gellan	0.26 ± 0.07	6.9 ± 0.3	0.29 ± 0.01
Gelatin-gellan with calcium	1.7 ± 0.7	6.1 ± 0.4	0.30 ± 0.04
Gelatin-5% gelatin	0.5 ± 0.3	7 ± 3	0.25 ± 0.04
Gelatin-10% gelatin	3.0 ± 0.4	10.5 ± 0.5	0.52 ± 0.01

2.3.2 Mechanical properties

To illustrate the effect of microgels on the mechanical properties of the matrix material after curing, tensile mechanical tests were carried out on gelatin-gellan composite hydrogel specimens. Although the primary purpose of the microgel component is to adjust the rheology of the precursor, it also has a marked effect on the properties of the cured hydrogel. Representative load/displacement curves for the two materials are shown in Figure 2(f). The effective stiffness of the filled and unfilled enzymatically cross-linked gelatin is significantly different. Although the stress-strain behavior in both cases is nonlinear, reasonable agreement between replicate samples of each type was observed. For illustration, the effective stiffness of the gelatin (3%) - gellan (0.5%), gelatin (3%) - gelatin (5%) and gelatin (3%) - gelatin (10%) composites is 14.9, 14.4, and 36.3 kPa, respectively, based on a linear approximation of the data collected after a 0.4 g preload is applied, making them handleable. The unfilled material is extraordinarily soft: extending specimens to approximately 300% strain (6 mm gage, 20 mm extension) exerted a barely measurable load on the test equipment so the apparent stiffness is less than 1 kPa. However, though soft, the unfilled matrix is quite elastic/resilient and mechanical behavior essentially similar over three stretching cycles.

The enhanced mechanical properties of the composite are consistent with literature; [34] stiff particles in a soft matrix form a stiffer composite. In addition, because of the preparation process, preformed microgels likely excluded gelatin. This would confine the gelatin to the free solvent volume between microgels and result in a much higher effective gelatin concentration between microgel particles, also increasing the mechanical stiffness. These two factors combine to result in a mechanically resilient, though still quite soft, hydrogel composite which can be intricately structured for functional objects. It should be noted that while the fabricated gelatin composite structures are quite soft, they are not particularly fragile so can be handled and manipulated easily. Many tissues are also quite soft: liver, brain, adipose, and other tissues have effective moduli in the same range (0.1 kPa to 1 MPa) as measured for the printed constructs. Encapsulated cells respond to the stiffness of their surroundings so it is an important characteristic for directing tissue development in engineered constructs.

4. Embedded Printing Results and Discussion

4.1 Printing procedure

As shown in Figure 1, the microgel particles are jammed at rest and cause the entire matrix bath material to behave as a solid. As the nozzle travels through the matrix bath, it locally liquefies the bath material by unjamming the surrounding gelatin solution. Thus, the liquefied composite matrix bath flows around the nozzle and the deposited ink, allowing the nozzle to move freely within the reservoir volume and permitting the sacrificial fluid ink to displace fluidized matrix bath material. As the nozzle moves away from a region, the jammed microgel particles revert to solid-like behavior, trapping the deposited ink in the designed configuration. After the printing process is complete, the continuous gelatin solution present between microgels is converted to a

chemically cross-linked hydrogel by the action of TG, as described previously. Finally, the sacrificial ink is liquefied and flushed if cross-linked during printing or directly flushed if uncross-linked from the cross-linked composite hydrogel matrix, leaving voids in the bulk hydrogel construct suitable for perfusion. The proposed method can also be expanded to sculpt external contours by discarding excess composite hydrogel matrix after printing and cross-linking. For such bulk objects defined by solid object sculpting, manual removal of excess cross-linked matrix to release the internal sculpted object is required instead of fluid flushing as the final step in the fabrication process.

4.2 Perfusable internal feature printing

Printed structures including twisted, branching, and interconnected channels formed by depositing sacrificial material in the gelatin-gellan and gelatin-gelatin matrix baths, respectively, were fabricated (Figure 3). Gelatin-gellan material is used for most examples, but representative patterns in gelatin-10% gelatin composite hydrogel matrices are also shown to illustrate comparable printing performance in other matrix bath formulations.

Twisted channels (Figure 3(a)) are designed to demonstrate the potential for truly 3D fluidic channels spanning multiple planes, which are difficult to achieve with other fabrication techniques and which enable more compact and efficient fluid handling as well as expanding the applications of microfluidic devices.[59] Each channel was printed intermittently as segments in order to be twisted. Due to die swelling and alginate diffusion, the printed channel diameter varies from 0.75 mm to 1.00 mm with a dispensing nozzle inner diameter of 0.84 mm. This design also shows other capabilities of the embedded printing process: planar segments can be

formed in a designed configuration, nonplanar segments can form continuous lumens with planar segments, segments printed at different stages in the fabrication process can be connected, and the feature size can be adjusted during printing. The elasticity of the matrix bath material makes results particularly sensitive to the print path design; corners and junctions tend to be distorted when printed at high speeds or when print paths cross in exactly the same plane. During printing, a small volume of support material surrounding the traveling nozzle is liquefied, so sharp corners are rounded if the nozzle travels too fast for the first segment to be trapped before the travel direction changes to deposit the second segment. Similarly, for in-plane path crossings, the liquefied region around the traveling tip unjams the matrix bath material around the previously deposited filament and distorts it as it travels across. This problem is mitigated by offsetting path crossings slightly in the z direction such that the bottom filament is largely intact but still fuses with the top filament. Intersections between channels printed during different steps, whether the segments form a fluidic junction or simply a continuous channel, must be designed with care; the moving nozzle disrupts a small volume of support material ahead of it so may prevent fusion of channels where the designed deposition paths only intersect at a single point. Instead, the print path should be designed such that the printing tip travels through the first filament as it deposits the second. In the twisted channel example, segments printed at different times in the fabrication process extend nominally 0.5 mm beyond the intersection point which results in excellent connectivity between segments and free flow of solutions and suspensions through the connected channels. Larger diameter wells for infusing solutions into the channels are formed by depositing small circular layers of sacrificial material rather than a simple post; this is an effective approach to create larger void volumes of specific shapes and sizes. It is noted that complicated and/or twisted channels can be achieved using alternative technologies such as casting[60] and

stereolithography,[61] however, it is difficult for casting to generate more complicated and twisted channels since a casting bioink may flush away slender sacrificial structures and for stereolithography to carve out channels out of a cell-laden matrix.

Figure 3(b) specifically illustrates the feasibility of branching channels with good connectivity formed by diverging print paths. In addition, planar structures suitable for microscopic examination are of interest for *in situ* observation of cells within printed constructs as well as fluid dynamics. The structure in Figure 3(c) adds a layer of complexity by combining multiple branches and two discrete perfusable channel systems within the same reservoir. The lattice network in Figure 3(d) is a simplified version of branching channels which are an essential feature of the vasculature; such orthogonal branching networks or lattices are often used to approximate vasculature in engineered constructs[21] since they are easier to design and model. More biomimetic hierarchical channel networks are also feasible, as shown in Figure 3(e). In general, printing performance is similar for gelatin-gelatin and gelatin-gellan matrix bath formulations; representative gelatin-gelatin composite constructs with printed features are shown in Figure 3(f) and (g).
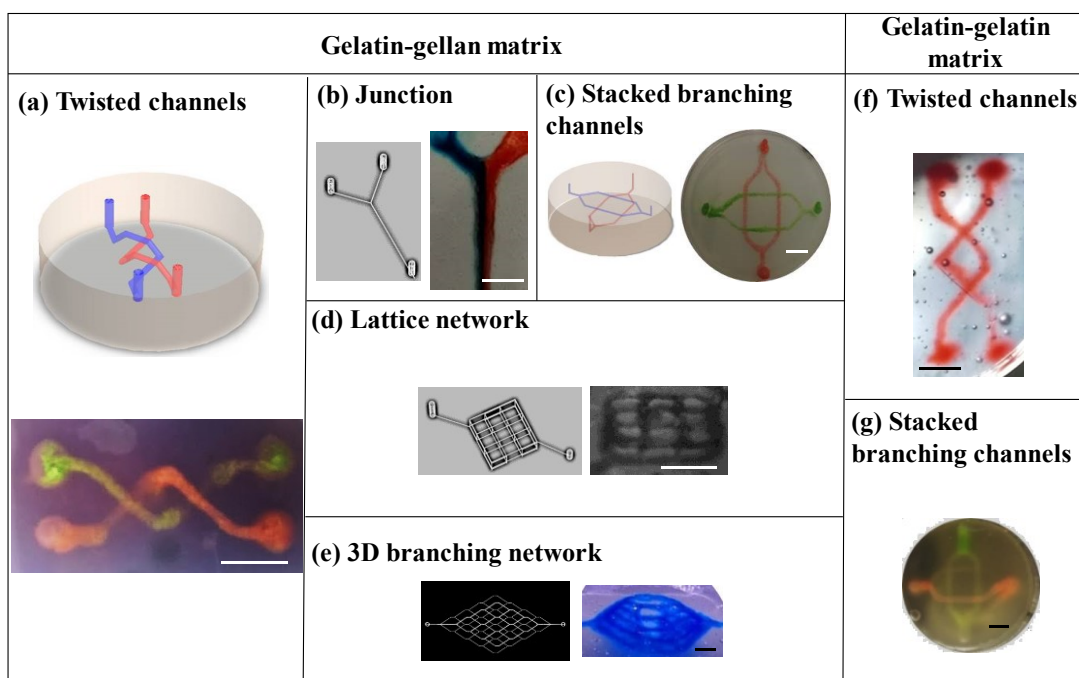
Figure 3. Printed internal features in gelatin-gellan (a-e) and gelatin-gelatin (f-g) composite matrices showing different channel geometries and designs. (Scale bars: 5 mm)

It is noted that matrix bath formulations may need to include calcium cations to partially cross-link sacrificial alginate ink in order to prevent excessive diffusion of the ink material from its printed location. Fortunately, it is unnecessary to include calcium cations for gelation for simple printed patterns, and similar printing performance is achieved for matrix formulations with and without calcium cations as shown in **Figure 4**.
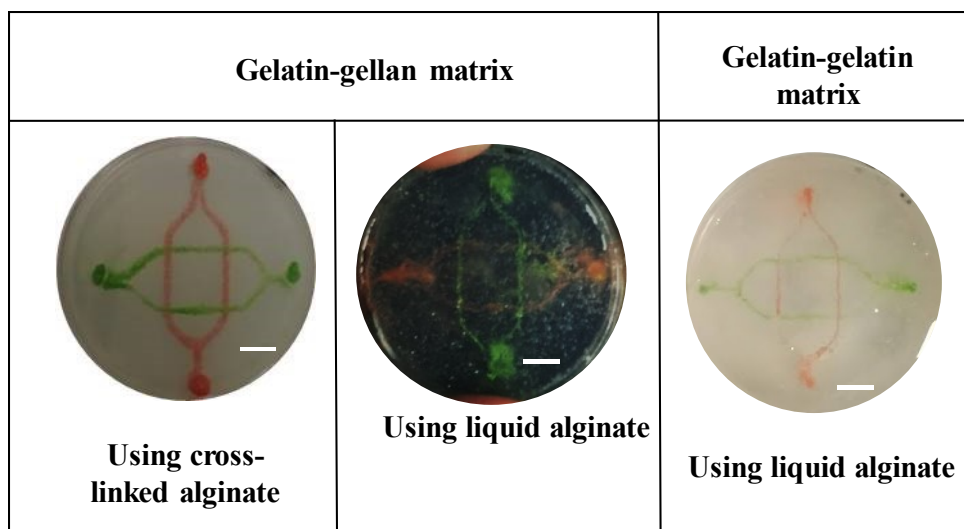
Figure 4. Printing performance with (using cross-linked alginate) and without (using liquid alginate) calcium in matrix bath formulations with printed sacrificial alginate patterns; images captured after rinsing away sacrificial ink and infusing channels with pigment. (Scale bars: 5 mm)

4.3 Solid object sculpting

As a special application, embedded printing also enables the production of solid objects as illustrated in **Figure 5**, by simply tracing the outer contour as a shell within a larger matrix bath reservoir (Figure 5(a-b)), then curing the matrix bath material (Figure 5(c)) and separating the region defined by the sacrificial ink from the excess material (Figure 5(d)). This sculpting process is a convenient method to generate freeform soft solid hydrogel structures from structural models and medical imagery. Dumbbell-shaped structures are fabricated to demonstrate that overhanging features and well defined edges and corners are feasible. They are formed by depositing a base layer to define the bottom surface, then depositing the walls and top surface layer by layer. The internal sculpted object cures concurrently with the external hydrogel

composite matrix, but is entirely isolated from it by the deposited sacrificial material. After curing, the excess material is simply cut or fractured to free the internal sculpted object, which can be rinsed to remove the fluid sacrificial material from the surface. To facilitate recovery of these embedded objects, a slit may be formed by adding a line of sacrificial material in each layer to create a wall extending into the excess bulk matrix bath region from the printed contour, as shown in Figure 5(a)-(c). After curing, this wall forms a slit in the composite hydrogel matrix which facilitates removal of excess material from the printed object (Figure 5(d)).

Although some matrix material is wasted in this solid object sculpting fabrication process, it enables rapid translation of arbitrary 3D shapes from computer models to solid hydrogel objects independent of orientation and without requiring the generation of support material or infill. For example, a 3D brain model was converted to G-code and printed within an hour, then cured and separated from the excess material to obtain an intact model replicating the intricate surface of the 3D model as shown in Figure 5(e). This makes it more accessible for non-expert users of 3D printing technology, especially since typical hydrogel printing processes require support bath materials or concurrent printing of mechanical reinforcements. It is noted that some hydrogels such as alginate can be printed into a simple gelation solution such as a calcium chloride solution for alginate and gels into a 3D structure, [10, 11, 62] but this approach only works for some hydrogels and certain thin-walled shapes, which can be easily supported and gelled during printing. Furthermore, the fabricated solid objects are truly homogeneous solids: there are no entrapped air bubbles between filaments, no layer interfaces, and no differences between perimeter and infill regions. Because the objects are isotropic, swelling or shrinkage due to post-processing conditions is also isotropic and does not cause structural failure or delamination.

It should be pointed out that solid object sculpting is a special application of embedded printing where embedded features can be combined to form biomedical constructs with both internal and external features. Block constructs with both external and internal features are designed and printed as shown in Figure 5(f). The blocks are formed by first printing the base, then depositing the walls and internal lattice concurrently, followed by vertical posts to connect features in different *xy* planes, and finally printing the top surface. The designed blocks have smooth outer walls along with periodic orthogonal channels forming an internal network. Cell-laden printed blocks are also feasible and the printed perfusable internal features have a notable influence on their biological activity as discussed later.
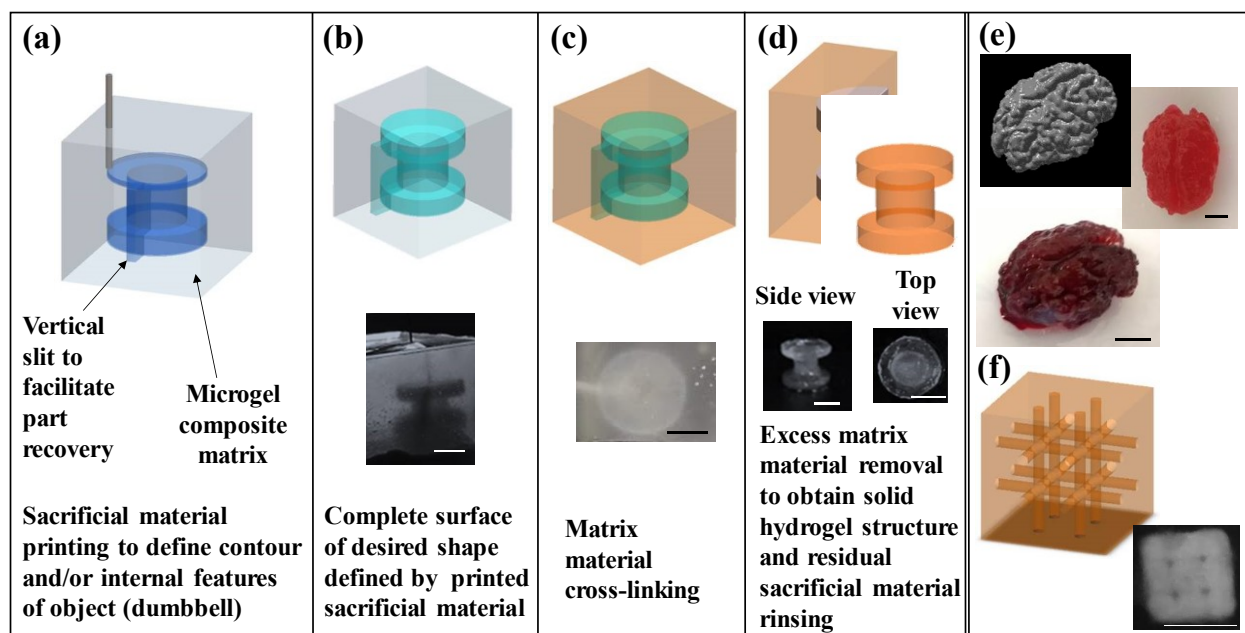
Figure 5. Embedded surface printing for solid object sculpting: (a) schematic of sacrificial material printing including slit to facilitate part harvesting, (b) complete exterior contour of dumbbell construct defined by a printed sacrificial material shell, (c) cured hydrogel composite block with embedded object contour, (d) removal of external composite hydrogel matrix material

to recover solid sculpted hydrogel object, and schematics and photos of other structures fabricated by solid object sculpting: (e) sculpted brain model based on medical imaging data and (f) sculpted lattice block with internal channels. (Scale bars: 5 mm).

4.4 Microgel composite matrix for cellular applications

The proposed composite matrix bath formulations are further evaluated for biocompatibility. Living cells embedded in the composite hydrogel matrix formulations are observed to spread and proliferate over time. To compare the biocompatibility and bioactivity of the various composite hydrogel matrix formulations, cast cell-laden discs were cultured and cell morphology was observed on Day 1, Day 3, and Day 7 using a fluorescein diacetate green stain for live cells, as shown in **Figure 6**(a). Unexpectedly, although the cells in the gelatin-gellan composite lagged in terms of cell extension and appeared round on Day 1, the cell population in the gellan composite appeared much more active and extended than the cell population in the gelatin-gelatin composite at Days 3 and 7. As observed elsewhere, gellan microgel composites provide a hospitable environment for 3D cell culture. [34] The lower cell activity in the gelatin-10% gelatin matrix is attributed to the overall high polymer concentration of ~13.0% (versus 3.5% in the gelatin-gellan composite), which reduces diffusion and therefore restricts cell nutrition and exposes them to elevated levels of metabolic waste products. The lower overall polymer concentration in the gelatin-gellan composite (3.5%) allows more effective diffusion and supports more extensive cell activity. Furthermore, patterning of heterogeneous cell populations can be achieved in a hydrogel composite construct using the proposed embedded printing approach as seen from Figure 6(b-d). First, a gelatin-gellan or gelatin-gelatin composite matrix bath is prepared as described earlier. Second, different cell populations are patterned in the yield-

stress composite matrix bath by depositing non-sacrificial cell-laden inks containing different cell types in specific locations within the matrix bath, resulting in a heterogeneous cellular pattern. The purple rings in Figure 6 are to distinguish different cellular rings from each other, and the blue color from Hoechst 33342 represents cell nuclei.
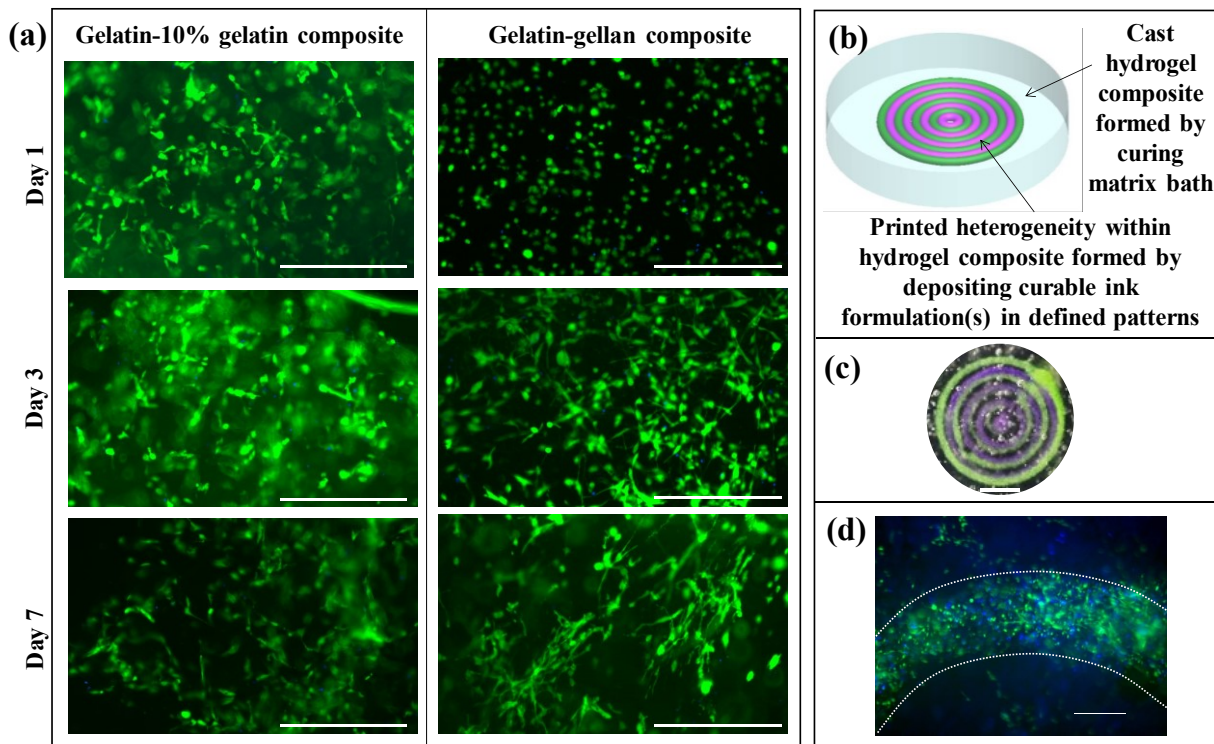

Figure 6. (a) Living cells within matrix formulations at various time points. Patterning of heterogeneous cell populations: (b) schematic of a heterogeneous construct, (c) pigment-laden ink pattern within a gelatin-gelatin hydrogel composite disc, and (d) part of a fluorescently stained cell-laden circle within an acellular gelatin-gelatin hydrogel composite disc. (Scale bars: 400 μm for (a), 5 mm for (c), and 500 μm for (d))

To demonstrate the feasibility in perfusable thick tissue fabrication using the proposed composite matrix bath formulations, cellular block constructs with embedded lattice channels, as shown schematically in Figure 5(f) and in the photographs in **Figure 7**(a), were printed and cultured statically for 4 days. Their metabolic activity and cell morphology are further compared with those of solid block constructs of the same composition (but lacking a printed lattice). The AlamarBlue assay results in Figure 7(b) show that the metabolic activity in printed constructs increased more rapidly than in solid blocks, indicating that the printed features improve cell activity. While the AlamarBlue assay results are affected by the surface area of the constructs as well as diffusion speed, it is a useful early metric for evaluating cell survival and activity within engineered tissue constructs. Cells which are unable to interact with the AlamarBlue assay reagents during the treatment period are also unlikely to survive for long since they are not able to access fresh media components. In future, more in-depth studies which examine markers of specific cell activities for tissue-specific functions need to be evaluated spatiotemporally to assess engineered tissue constructs. Cross sections from the interior of the block are stained to observe green fluorescence from living cells and evaluate whether printed channel features improve cell survival within bulk cellular constructs. Although live cells are present in both printed and cast hydrogel constructs, they appear more abundant in printed structures, with extensive spreading as well as developing clusters of cells due to proliferation. Representative images of central cross sections (showing regions away from the edges of the blocks) are shown in Figure 7(c) and (d). In particular, a perfusion channel is visible in Figure 7(c).
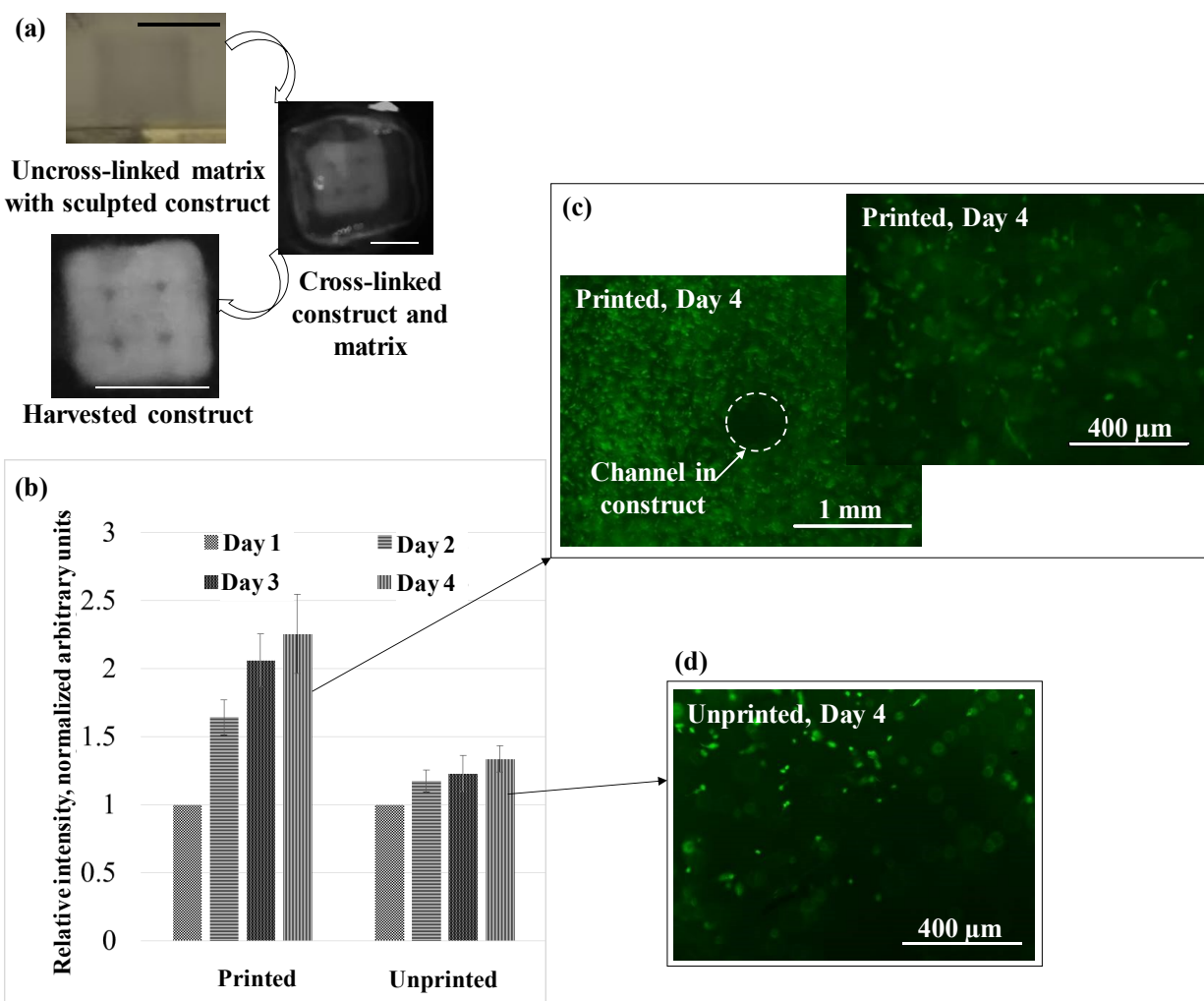
Figure 7. Cellular gelatin-gellan constructs (a) images of overall printed constructs and cell populations within printed and unprinted constructs, (b) cell activity in printed and unprinted constructs, and (c) and (d) living cell images on Day 4. (Scale bars: 5 mm unless otherwise marked)

4.5 Printing quality and design constraints

There are two major factors which affect the outcome of a printing process: the composite material selection and the printing parameters.

4.5.1 Effects of composite material on printing quality

The rheological properties of the matrix bath shift during the printing process as the added TG begins to cross-link the matrix bath, transforming the yield stress precursor to a covalently cross-linked composite hydrogel matrix. As a result, the printing performance also changes. This was assessed by printing channels at timed intervals after the addition of TG to the matrix bath, then curing and sectioning the gel block to observe the channel morphology. A gradual shift from perfectly round (aspect ratio of 1.066 and roundness of 0.938) to significantly elongated (aspect ratio of 2.057 and roundness of 0.486) channels was observed from immediately after mixing TG into the gelatin-gellan matrix bath to 40 minutes after mixing as shown in **Figure 8**; after this time, attempting to print in the partially cured matrix bath caused tearing as the matrix material deformed elastically and eventually fractured rather than flowing around the traveling nozzle. Deposited sacrificial material did not form well defined features under these conditions, as indicated by the large error bars at late time points in Figure 8. Allowing 5 minutes for loading the TG-supplemented matrix material in the reservoir and assuming a speed of 150 mm/min, it is possible to print over 5 m of sacrificial material before the performance deteriorates significantly (35 min × 150 mm/min = 5250 mm = 5.25 m). This translates, for example, to a 1×2×2 cm construct with no cell further than 200 μm from a 600 μm diameter printed channel.
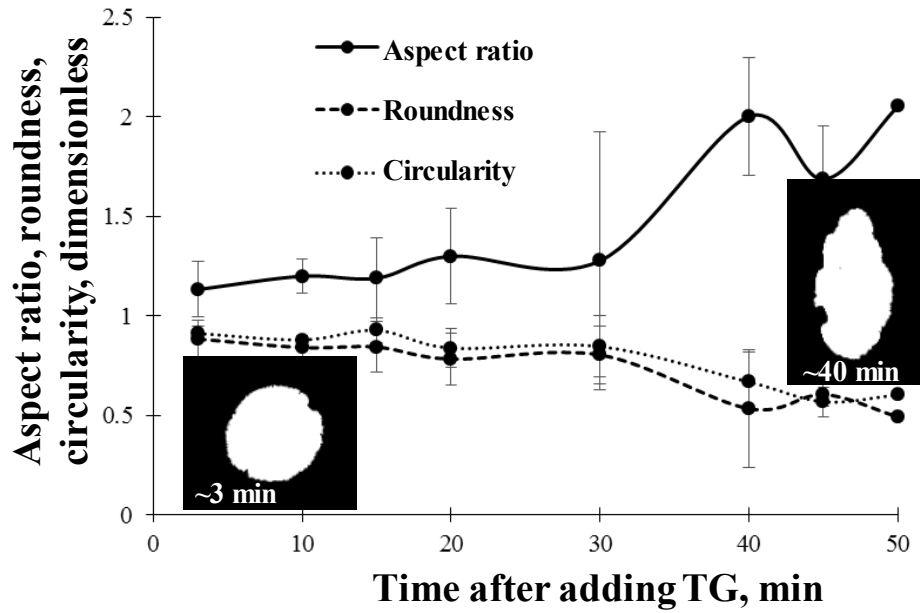
Figure 8. Effects of changing rheological properties on printed channel morphology (0.5%

gellan + 3% gelatin and 0.5% TG)

4.5.2 Effects of fabrication parameters on printing quality

Generally, the printing resolution (minimum channel size in this study) depends on the

dispensing nozzle tip size and printing conditions/parameters, and the feature morphology

(channels in this study) is influenced by the printing time and varying yield-stress property of the

matrix bath. Herein, the minimum channel size is primarily controlled by the nozzle tip diameter

in this displacement-based printer where the flow rate is automatically adjusted to match the

travel speed in order to maintain the filament width; however, larger circular channels can be

produced by either using a larger nozzle tip or printing sacrificial materials atop of each other

along the same print path. Attempts to print small channels using a low flow rate through a

relatively large tip resulted in poorly-shaped (but intact) channels; the cross section was

triangular due to the wide void space created behind the tip and resulting up overflow of the

sacrificial material. In general, the shape of the channel cross section deteriorates over the course of the printing process as the matrix material's recovery behind the tip becomes slower and less complete, as discussed in the previous section. This may be observed during printing as an increasing tendency of the matrix bath around the tip to deform elastically rather than simply flow around it. After printing, the most noticeable effect of longer print time is a transition to vertically elongated or tear-drop shaped channel cross sections, in contrast to the ideal circular cross section of features printed immediately after matrix preparation. The 'printing window' is defined as the longest time after matrix preparation when reasonably circular cross sections are observed, and is approximately 35 min herein. The minimum gap between channels is similar in both the *xy* plane and for vertical *z* stacking, and is approximately equal to the filament width.

These results are comparable to those achieved using previously reported materials[28,30,31] for embedded printing: minimum channel size is set by the tip size and can be adjusted by altering the flow rate or travel speed. An analogous process utilizes focused radiation (typically laser light) to selectively ablate material within a hydrogel monolith, creating cavities, channels, and other features[63]. While valuable in some contexts, especially where creating void space in a precise spatial arrangement relative to existing cells is needed, the low throughput and low penetration depth of this technique limits its utility for larger structures. Embedded printing, however, enables rapid fabrication of fluidic networks through the entire volume of thick structures.

5. Conclusions

This report evaluates the use of a microgel-filled cross-linkable yield stress composite hydrogel as a matrix bath to enable embedded patterning of sacrificial materials to generate engineered tissue constructs with perfusable internal channels. The combination of yield-stress fluid behavior from a jammed microgel filler (such as gellan or gelatin) and susceptibility to covalent cross-linking from the continuous phase (the gelatin and TG mixture herein) enables rapid custom fabrication of mechanically robust perfusable engineered constructs laden with cells. This approach has potential for both *in vitro* and *in vivo* applications and may be especially useful for chip-based systems where traditional printing methods would have difficulty depositing a cell-laden matrix to completely fill a pre-existing cavity. Both 2D and 3D fluidic networks have been demonstrated using the proposed composite matrix bath. Networked channels increase the metabolic activity of living cells in the cross-linked matrix. The bath temperature for printing and during incubation has been maintained at 37°C, and a temperature lower than 37°C may cause the physical gelation of gelatin and negatively affect the printing process.

In addition, the yield stress microgel composite matrix bath also enables solid object sculpting by printing a shell of sacrificial material to define the external contour of an object in a composite matrix bath as well as patterning of heterogeneous cell populations within a bulk construct. This solid object sculpting method may be particularly useful for generating patient-specific models with properties analogous to native tissue to aid in medical training and facilitate surgical planning; custom implantable printed constructs may also be readily fabricated based on medical imaging of specific tissue defects. Soft constructs which combine internal heterogeneity and

custom outer contours may also be valuable in surgical planning. The ability to control the spatial arrangement of heterogeneous cell populations within engineered constructs is another invaluable application of this methodology; tissue functionality depends on the coordinated efforts of specialized cells in specific spatial arrangements relative to one another. Engineered tissues which recapitulate this spatial organization to match native tissue are of great interest for both clinical applications and studying the relationship between tissue structure and functionality.

It should be noted that the main contribution of this study is to design and test a cross-linkable microgel composite matrix bath for embedded bioprinting of perfusable tissue constructs as well as sculpting of solid objects. The microgel composite-based matrix bath material forms the final construct. As such, the selection of the best sacrificial materials and the printing of most delicate channels are not the focus of this study. While aqueous alginate solution is used as a sacrificial ink, more advanced sacrificial materials can be utilized for better printing resolution. For the creation of deep microscale channels, the sacrificial material should be chosen less viscous during removal, and the gelled matrix should be designed to have enough mechanical strength to maintain its mechanical integrity during sacrificial material removal.

Future work may include additional cell studies and material optimization for dynamic thick tissue perfusion and specific tissue engineering applications such as fracture strength for suturing, exploration of alternative microgel and/or continuous phase materials to adjust the mechanical properties, the effects of matrix curing and printing conditions/time, and functional properties of the printed objects such as the diffusion limit of perfused materials, better imaging

quality of printed channels, and better characterization and understanding of rheological properties of various microgel composite matrix baths. Specifically, a detailed chemical analysis of the matrix bath cross-linking process should be characterized and related to the bath rheological properties and duration of printable time, the boundary condition between the matrix and microgel particles needs to be characterized using an environmental scanning electron microscope since there may be some cross-linking reactions due to the TG in the gelatin continuous phase; and the design and fabrication of vasculatures with complicated structures should be pursued by optimizing the sacrificial material as well as the microgel for the composite matrix bath.

6. Materials and Methods

6.1 Material preparation

6.1.1 Gelatin-gellan matrix bath

The gelatin-gellan matrix bath material was prepared by dissolving 3% w/v gelatin and 6.8 mM $CaCl_2$ (0.1% w/v $CaCl_2\cdot2H_2O$) as needed in jammed 0.5% w/v gellan microgels, then adding transglutaminase. Gellan microgel dispersions were prepared by following a published protocol.[17] Then, the appropriate mass of gelatin (225 bloom, type A, from porcine skin, MP Biomedicals, Solon, OH) and calcium chloride (calcium chloride dihydrate, Sigma-Aldrich, St. Louis, MO) as needed was added to the jammed microgels and allowed to dissolve at 37°C until a clear mixture was obtained. To enable rapid and efficient addition of TG to the matrix mixture, a 20 wt% stock solution of tranglutaminase (MooGloo TI, Modernist Pantry, York, ME) was prepared by dissolving the dry powder in PBS; the mixture was vortexed briefly and maintained at 37°C for 20 minutes to dissolve the enzyme, then stored at 4°C until use. Immediately before

printing, TG stock was added to the warm matrix mixture for a final concentration of 0.5 wt%. The warm mixture was gently mixed and centrifuged to remove bubbles before loading in the print bath for patterning. Immediately after loading the matrix material (0.5% gellan, 3% gelatin, 0.5% TG, and 6.8 mM $CaCl_2$ as needed) in the print reservoir, the reservoir was placed on the heated print bed and the sacrificial ink was deposited to create features within the material. After the printing process was complete, the print reservoir was held at 37°C for 75 minutes for full cross-linking.

6.1.2 Gelatin-gelatin matrix bath

Gelatin microgels were prepared by fragmenting a bulk covalently cross-linked gel. Gelatin was dissolved in PBS at 37°C to make a 22.2% w/v solution. A 20% w/v stock solution of TG (Moo Gloo TI, Modernist Pantry, York ME) in PBS was prepared separately by dispersing the powder in PBS, vortexing briefly, then incubating at 37°C for 20 minutes; TG stock was stored at 4C for up to one week before use. The two solutions were mixed at a 9:1 ratio for final concentrations of 20% gelatin and 2% TG, and incubated for 4 hr at 37°C for gel formation in a conical vial. 5% and 10% w/v gelatin gels were prepared analogously, keeping the 10:1 ratio between gelatin and TG constant (that is, they were cross-linked using 0.5% and 1.0% TG respectively). The vial of covalently cross-linked gel was then placed in boiling water for 20 min to deactivate TG. Finally, the bulk gel was placed in a beaker with deionized water for a total volume of ~200 mL and fragmented using a household immersion blender on high for 5 min. Excess water was removed by centrifuging the microgel mixture (5 min at 4200 rpm) and discarding the watery supernatant; the packed microgels were then stored at 4°C until use.

In addition, the covalently cross-linked gelatin microgels were also autoclaved at 121°C for 60 min to prepare materials for cell culture; excess PBS was added prior to autoclaving to prevent desiccation of the microgels, and they were re-collected by centrifuging after sterilization.

Gelatin composites were prepared by combining dry gelatin with gelatin microgels. Typically, 0.3 g gelatin was combined with 10.0 g gelatin microgels to make a composite curable matrix precursor. As needed, 6.8 mM $CaCl_2$ was added for alginate gelation. The mixture was warmed to 37°C and mixed thoroughly until homogeneous, then combined with TG stock immediately before printing.

6.1.3 Sacrificial ink

The alginate-based sacrificial ink was prepared by dissolving 2% w/v high-molecular weight alginate (Acros Organics, Waltham MA) in PBS.

6.1.4 Cell-laden matrix

NIH 3T3 fibroblasts were harvested as previously described, [9] pelleted, and resuspended for this work. For biocompatibility assessment and cell patterning studies, cells were resuspended in the warm gelatin- gelatin matrix bath mixture before adding TG stock solution. For morphology evaluation, the cell-laden matrix was cast in a 24-well plate. For cell patterning, the cell-laden matrix was loaded in a sterilized syringe for dispensing into a cast acellular matrix bath.

For printed cell-laden structures, cell were resuspended in the warm gelatin-gellan matrix bath mixture with calcium at 2.5×10^6 cells/ mL just before adding the TG stock solution. Cellular

structures were printed with a 30 gauge tip. To verify that cells remained viable and that the matrix supported adhesion and cellular interactions, 5 mm thick cast discs of the cell laden matrix material without printed features were initially fabricated and cultured for several days. Cell-laden structures were incubated in complete culture media (Dulbecco's modified Eagle's medium (DMEM, Sigma-Aldrich, St. Louis, MO) with 10% Fetal Bovine Serum (FBS) (HyClone, Logan, UT)) in a humidified 5% CO_2 incubator. Metabolic activity was assessed on 1, 2, 3, and 4 using the alamarBlue assay (ThermoFisher Scientific, Waltham, MA) according to the manufacturer's instructions except that the incubation time was extended to 6 hours; fluorescent intensity was recorded using a plate reader (Synergy HT, Biotek, Winooski, VT). Cellular constructs were stained with fluorescein diacetate (FDA) (green) for live cells and/or Hoechst 33342 (blue) for nuclei using a protocol in a previous study.[17]

6.2 Matrix characterization

6.2.1 Rheology measurement

Rheological properties were measured as previously described [17]. In particular, samples were subjected to a preshear step (100 s^{-1} for 30 sec) followed by a 60 sec recovery period to eliminate loading effects.

6.2.2 Mechanical properties

The effect of the gellan microgel filler on the mechanical properties of the covalent gelatin gel were evaluated using tensile mechanical tests. Dogbone shaped samples of either the print matrix, prepared as described in 4.1.1, or gellan-free 3% gelatin in PBS with 0.5% TG, were cast in PDMS molds. The molds were prepared from machined aluminum masters and had

dimensions of 0.50 thick × 1.25 wide × 6.00 long (all in mm); the hydrogel precursors were allowed to cure at 37°C for 60 minutes, then carefully demolded and immediately tested as described in a previous study.[17] Data was exported to Microsoft Excel for further processing.

6.3 Printing and design constraints

For printing, a Hyrel Engine SR 3D printer (Hyrel3D, Norcross, GA) was utilized as described in a previous study.[17] Although exact settings varied slightly, the layer height setting was typically ~0.5× the nozzle width, and the print speed was set at 2.5-5 mm/sec in the x and y directions and 2.5 mm/sec in the z direction.

6.4 Post-processing

After printing, constructs with embedded sacrificial ink were allowed to cross-link at 37°C for 45 min. Then, the sacrificial ink was removed from channels or the sculpted objects were separated manually from excess matrix material. In cases where the sacrificial material did not form a gel (alginate in calcium-free matrix formulations), the fluid sacrificial material was simply flushed from internal channels by infusing water (acellular constructs) or PBS (cell-laden constructs). For alginate sacrificial ink in calcium-containing matrix formulations, soaking in 1.62% w/v sodium citrate (molecular biology grade, BDH, USA) for several hours was necessary to fully liquefy the sacrificial ink within perfusable features so that they could be flushed with other fluids. Sculpted objects were recovered by simply manually separating the internal sculpted object from excess matrix material; soaking in citrate facilitated this process when alginate sacrificial ink was used with calcium-containing matrix formulations, but was not essential.

Acknowledgements

Competing financial interests

This work has been disclosed to the Office of Technology Licensing at the University of Florida.

Data availability

The raw/processed data required to reproduce these findings cannot be shared at this time as the data also forms part of an ongoing study.

References

(1) Murphy, S.V.; Atala, A. 3D Bioprinting of Tissues and Organs Nature Biotechnology 2014, 32, 773.

(2) Huang, Y.; Leu. M.C.; Mazumder, J.; and Donmez, A. Additive Manufacturing: Current State, Future Potential, Gaps and Needs, and Recommendations ASME Journal of Manufacturing Science and Engineering 2015, 137, 014001.

(3) Lee, J.M.; Yeong, W.Y. Design and Printing Strategies in 3D Bioprinting of Cell-Hydrogels: A Review Advanced Healthcare Materials 2016, 5, 2856-2865.

(4) Lee, V.K.; Dai, G. Printing of Three-Dimensional Tissue Analogs for Regenerative Medicine Annals of Biomedical Engineering 2017. 45, 115-131.

(5) Richards, D.; Jia, J.; Yost, M.; Markwald, R.; Mei, Y. 3D Bioprinting for Vascularized Tissue Fabrication Annals of Biomedical Engineering 2017, 45, 132-147.

(6) Huang, Y.; Schmid, S. Additive Manufacturing for Health: State of the Art, Gaps and Needs, and Recommendations Journal of Manufacturing Science and Engineering 2018, 40, 094001.

(7) Zhang, Z.; Jin, Y.; Yin, J.; Xu, C.; Xiong, R.; Christensen, K.; Ringeisen, B.R.; Chrisey, D.B.; Huang, Y. Evaluation of Bioink Printability for Bioprinting Applications Applied Physics Reviews 2018, 5, 041304-1-21.

(8) Shih, A.J.; Li, W., Huang, Y. Chapter 9: Biomedical Manufacturing, in Handbook of Manufacturing edited by Yong Huang, Lihui Wang, and Steven Y. Liang, World Scientific Publishing, Singapore, 2019.

(9) Xu, C.; Chai, W.; Huang, Y.; Markwald, R.R. Scaffold-Free Inkjet Printing of Three-Dimensional Zigzag Cellular Tubes Biotechnology and Bioengineering 2012, 109, 3152-3160.

(10) Christensen, K.; Xu, C.; Chai, W.; Zhang, Z.; Fu, J.; Huang, Y. Freeform Inkjet Printing of Cellular Structures with Bifurcations Biotechnology and Bioengineering 2015, 112, 1047-1055.

(11) Xiong, R.; Zhang, Z.; Chai, W.; Huang, Y.; Chrisey, D.B. Freeform Drop-on-Demand Laser Printing of 3D Alginate and Cellular Constructs Biofabrication 2015, 7, 045011.

(12) Hinton, T.J.; Jallerat, Q.; Palchesko, R.N.; Park, J.H.; Grodzicki, M.S.; Shue, H.J.; Ramadan, M.H.; Hudson, A.R.; Feinberg, A.W. Three-Dimensional Printing of Complex Biological Structures by Freeform Reversible Embedding of Suspended Hydrogels Science Advances 2015, 1, e1500758.

(13) Jin, Y.; Compaan, A.; Bhattacharjee, T.; Huang, Y. Granular Gel Support-Enabled Extrusion of Three-Dimensional Alginate and Cellular Structures Biofabrication 2016, 8, 025016.

(14) Jin, Y.; Chai, W.; Huang, Y. Printability Study of Hydrogel Solution Extrusion in Nanoclay Yield-Stress Bath During Printing-Then-Gelation Biofabrication Materials Science and Engineering: C 2017, 80, 313-325.

(15) Jin, Y.; Compaan, A.; Chai, W.; Huang, Y. Functional Nanoclay Suspension for Printing-Then-Solidification of Liquid Materials ACS Applied Materials & Interfaces 2017, 9, 20057-20066.

(16) Moxon, S.R.; Cooke, M.E.; Cox, S.C.; Snow, M.; Jeys, L.; Jones, S.W.; Smith, A.M.; Grover, L.M. Suspended Manufacture of Biological Structures Advanced Materials 2017, 29, 1605594.

(17) Compaan, A.M.; Song, K.; Huang, Y. Gellan Fluid Gel as a Versatile Support Bath Material for Fluid Extrusion Bioprinting ACS Applied Materials & Interfaces 2019, 11, 5714-5726.

(18) Miller, J.S.; Stevens, K.R.; Yang, M.T.; Baker, B.M.; Nguyen, D.H.T.; Cohen, D.M.; Toro, E.; Chen, A.A.; Galie, P.A.; Yu, X.; Chaturvedi, R. Rapid Casting of Patterned Vascular Networks for Perfusable Engineered Three-Dimensional Tissues Nature Materials 2012, 11, 768.

(19) Van Hoorick, J.; Declercq, H.; De Muynck, A.; Houben, A.; Van Hoorebeke, L.; Cornelissen, R.; Van Erps, J.; Thienpont, H.; Dubruel, P.; Van Vlierberghe, S. Indirect Additive Manufacturing as an Elegant Tool for the Production of Self-Supporting Low Density Gelatin Scaffolds Journal of Materials Science: Materials in Medicine 2015, 26, 247.

(20) Mohanty, S.; Larsen, L.B.; Trifol, J.; Szabo, P.; Burri, H.V.R.; Canali, C.; Dufva, M.; Emnéus, J.; Wolff, A. Fabrication of Scalable and Structured Tissue Engineering Scaffolds Using Water Dissolvable Sacrificial 3D Printed Moulds Materials science and engineering: C 2015, 55, 569-578.

(21) Kolesky, D.B.; Homan, K.A.; Skylar-Scott, M.A.; Lewis, J.A. Three-Dimensional Bioprinting of Thick Vascularized Tissues Proceedings of the National Academy of Sciences 2016, 113, 3179-3184.

(22) Parekh, D.P.; Ladd, C.; Panich, L.; Moussa, K.; Dickey, M.D. 3D Printing of Liquid Metals as Fugitive Inks for Fabrication of 3D Microfluidic Channels Lab on a Chip 2016, 16, 1812-1820.

(23) Yang, L.; Shridhar, S.V.; Gerwitz, M.; Soman, P. An In Vitro Vascular Chip Using 3D Printing-Enabled Hydrogel Casting Biofabrication 2016, 8, 035015.

(24) Jin, Y.; Chai, W.; Huang, Y. Fabrication of Stand-Alone Cell-Laden Collagen Vascular Network Scaffolds Using Fugitive Pattern-Based Printing-Then-Casting Approach ACS Applied Materials & Interfaces 2018, 10, 28361-28371.

(25) Wu, W.; DeConinck, A.; Lewis, J.A. Omnidirectional Printing of 3D Microvascular Networks Advanced Materials, 2011, 23, H178-H183.

(26) Mohanty, S.; Larsen, LB.; Trifol, J.; Szabo, P.; Burri, HV.; Canali, C.; Dufva, M.; Emnéus, J.; Wolff, A. Fabrication of Scalable and Structured Tissue Engineering Scaffolds using Water Dissolvable Sacrificial 3D Printed Moulds Materials Science and Engineering: C, 2015, 55, 569-578.

(27) Pimentel, C.R.; Ko, S.K.; Caviglia, C.; Wolff, A.; Emnéus, J.; Keller, S.S.; Dufva, M. Three-dimensional Fabrication of Thick and Densely Populated Soft Constructs with Complex and Actively Perfused Channel Network Acta Biomaterialia 2018, 65, 174-184.

(28) Ringeisen, B.R.; Pirlo, R.K.; Wu, P.K.; Boland, T.; Huang, Y.; Sun, W.; Hamid, Q.; Chrisey, D.B. Cell and Organ Printing Turns 15: Diverse Research to Commercial Transitions MRS Bulletin 2013, 38, 834-843.

(29) Hong, S.; Song, S.J.; Lee, J.Y.; Jang, H.; Choi, J.; Sun, K.; Park, Y. Cellular Behavior in Micropatterned Hydrogels by Bioprinting System Depended on the Cell Types and Cellular Interaction Journal of bioscience and bioengineering 2013, 116, 224-230.

(30) Highley, C.B.; Rodell, C.B.; Burdick, J.A. Direct 3D Printing of Shear-Thinning Hydrogels into Self-Healing Hydrogels Advanced Materials 2015, 27, 5075-5079.

(31) Shi, L.; Carstensen, H.; Hölzl, K.; Lunzer, M.; Li, H.; Hilborn, J.; Ovsianikov, A.; Ossipov, D.A. Dynamic Coordination Chemistry Enables Free Directional Printing of Biopolymer Hydrogel Chemistry of Materials 2017, 29, 5816-5823.

(32) Shin, S.; Hyun, J. Matrix-Assisted Three-Dimensional Printing of Cellulose Nanofibers for Paper Microfluidics ACS Applied Materials & Interfaces 2017, 9, 26438-26446.

(33) Grosskopf, A.K.; Truby, R.L.; Kim, H.; Perazzo, A.; Lewis, J.A.; Stone, H.A. Viscoplastic Matrix Materials for Embedded 3D Printing ACS Applied Materials & Interfaces 2018, 10, 23353–23361

(34) Lippens, E.; Swennen, I.; Gironès, J.; Declercq, H.; Vertenten, G.; Vlaminck, L.; Gasthuys, F.; Schacht, E.; Cornelissen, R. Cell Survival and Proliferation After Encapsulation in a Chemically Modified Pluronic® F127 Hydrogel Journal of Biomaterials Applications 2013, 27, 828-839.

(35) Han, L.H.; Lai, J.H.; Yu, S.; Yang, F. Dynamic Tissue Engineering Scaffolds with Stimuli-Responsive Macroporosity Formation Biomaterials 2013, 34, 4251-4258.

(36) Ferris, C.J.; Gilmore, K.J.; Beirne, S.; McCallum, D.; Wallace, G.G. Bio-Ink for On-Demand Printing of Living Cells Biomaterials Science 2013, 1, 224-230.

(37) Liu, G.; Pareta, R.A.; Wu, R.; Shi, Y.; Zhou, X.; Liu, H.; Deng, C.; Sun, X.; Atala, A.; Opara, E.C.; Zhang, Y. Skeletal Myogenic Differentiation of Urine-Derived Stem Cells and

Angiogenesis using Microbeads Loaded with Growth Factors Biomaterials 2013, 34, 1311-1326.

(38) Henry, N.; Clouet, J.; Fragale, A.; Griveau, L.; Chédeville, C.; Véziers, J.; Weiss, P.; Le Bideau, J.; Guicheux, J.; Le Visage, C. Pullulan Microbeads/Si-HPMC Hydrogel Injectable System for the Sustained Delivery of GDF-5 and TGF-β1: New Insight into Intervertebral Disc Regenerative Medicine Drug Delivery 2017, 24, 999-1010.

(39) Shin, H.; Olsen, B.D.; Khademhosseini, A. Gellan Gum Microgel-Reinforced Cell-Laden Gelatin Hydrogels Journal of Materials Chemistry B 2014, 2, 2508-2516.

(40) Miller, J.S.. The Billion Cell Construct: Will Three-Dimensional Printing Get us There? PLoS Biology 2014, 12, e1001882.

(41) Prajapati, V.D.; Jani, G.K.; Zala, B.S.; Khutliwala, T.A. An Insight into the Emerging Exopolysaccharide Gellan Gum as a Novel Polymer Carbohydrate Polymers 2013, 93, 670-678.

(42) Stevens, L.R.; Gilmore, K.J.; Wallace, G.G. Tissue Engineering with Gellan Gum Biomaterials Science 2016, 4, 1276-1290.

(43) García, M.C.; Alfaro, M.C.; Muñoz, J. Rheology of Sheared Gels Based on Low Acyl-Gellan Gum Food Science and Technology International 2016, 22, 325-332.

(44) Yang, G.; Xiao, Z.; Long, H.; Ma, K.; Zhang, J.; Ren, X.; Zhang, J. Assessment of the Characteristics and Biocompatibility of Gelatin Sponge Scaffolds Prepared by Various Crosslinking Methods Scientific Reports 2018, 8, 1616.

(45) Chen, P.Y.; Yang, K.C.; Wu, C.C.; Yu, J.H.; Lin, F.H.; Sun, J.S. Fabrication of Large Perfusable Macroporous Cell-Laden Hydrogel Scaffolds Using Microbial Transglutaminase Acta Biomaterialia 2014, 10, 912-920.

(46) Irvine, S.A.; Agrawal, A.; Lee, B.H.; Chua, H.Y.; Low, K.Y.; Lau, B.C.; Machluf, M.; Venkatraman, S. Printing Cell-Laden Gelatin Constructs by Free-Form Fabrication and Enzymatic Protein Crosslinking Biomedical Microdevices 2015, 17, 16.

(47) Moné, M.J.; Volker, M.; Nikaido, O.; Mullenders, L.H.; van Zeeland, A.A.; Verschure, P.J.; Manders, E.M.; van Driel, R. Local UV‑Induced DNA Damage in Cell Nuclei Results in Local Transcription Inhibition EMBO Reports 2001, 2, 1013-1017.

(48) Gedik, C.M.; Ewen, S.W.B.; Collins, A.R.; Single-cell Gel Electrophoresis Applied to the Analysis of UV-C Damage and its Repair in Human Cells International Journal of Radiation Biology 1992, 62, 313-320.

(49) Leena, L.; Laiho, M. Cellular UV Damage Responses—Functions of Tumor Suppressor p53 Biochimica Biophysica Acta. 2005, 1755, 71-89.

(50) Nury, S1.; Meunier, J.C.; Mouranche, A. The Kinetics of the Thermal Deactivation of Transglutaminase from Guinea‑Pig Liver European Journal of Biochemistry 1989, 180, 161-166.

(51) Im, M.J.; Russell, M.A.; Feng, J.F. Transglutaminase II: a New Class of GTP-binding Protein With New Biological Functions Cellular Signalling 1997, 9, 477-482.

(52) Shin, H.; Olsen, B.D.; Khademhosseini, A. The Mechanical Properties and Cytotoxicity of Cell-Laden Double-Network Hydrogels Based on Photocrosslinkable Gelatin and Gellan Gum Biomacromolecules Biomaterials 2012, 33, 3143-3152.

(53) Chilvers, G.R.; Morris, V.J. Coacervation of Gelatin-Gellan Gum Mixtures and Their Use in Microencapsulation Carbohydrate Polymers 1987, 7, 111-120.

(54) Mouser, V.H.; Melchels, F.P.; Visser, J.; Dhert, W.J.; Gawlitta, D.; Malda, J. Yield Stress Determines Bioprintability of Hydrogels Based on Gelatin-Methacryloyl and Gellan Gum for Cartilage Bioprinting Biofabrication 2016, 8, 035003.

(55) Dong, Z.J.; Xia, S.Q.; Hua, S.; Hayat, K.; Zhang, X.M.; Xu, S.Y. Optimization of Cross-Linking Parameters during Production of Transglutaminase-Hardened Spherical Multinuclear Microcapsules by Complex Coacervation Colloids and Surfaces B: Biointerfaces 2008, 63, 41-47.

(56) Xia, Y.; Zhang, X.; Bo, A.; Sun, J.; Li, M. Sodium Citrate Inhibits the Proliferation of Human Gastric Adenocarcinoma Epithelia Cells Oncology Letters 2018, 15, 6622-6628.

(57) Romano, N.; Simon, W.; Ebrahimi, M.; Fadel, A.H.I.; Chong, C.M.; Kamarudin, M.S. Dietary Sodium Citrate Improved Oxidative Stability in Red Hybrid Tilapia (Oreochromis Sp.) but Reduced Growth, Health Status, Intestinal Short Chain Fatty Acids and Induced Liver Damage Aquaculture 2016, 458, 170-176.

(58) Adams, S.; Frith, W.J.; Stokes, J.R. Influence of Particle Modulus on the Rheological Properties of Agar Microgel Suspensions Journal of Rheology 2004, 48, 1195-1213.

(59) Bhargava, K.C.; Thompson, B.; Malmstadt, N. Discrete Elements for 3D Microfluidics Proceedings of the National Academy of Sciences 2014, 111, 15013-15018.

(60) Keigo, N.; Mori, N.; Morimoto, Y.; Takeuchi, S. Formation of Vessel-Like Channel using Alginate Fiber as a Sacrificial Structure 2017 Proc. IEEE 30th International Conference on Micro Electro Mechanical Systems (MEMS) 2017 596-599.

(61) Grigoryan, B.; Paulsen, S.J.; Corbett, D.C.; Sazer, D.W.; Fortin, C.L.; Zaita, A.J.; Greenfield, P.T.; Calafat, N.J.; Gounley, J.P.; Ta, A.H.; Johansson, F.; Randles, A.; Rosenkrantz, J.E.; Louis-Rosenberg, J.D.; Galie, P.A.; Stevens, K.R.; Miller, J.S.

Multivascular Networks and Functional Intravascular Topologies within Biocompatible Hydrogels Science 2019, 364, 458-464.

(62) Xu, C.; Zhang, Z.; Christensen, K.; Huang, Y.; Fu, J.; Markwald, R. Freeform Vertical and Horizontal Fabrication of Alginate-Based Vascular-Like Tubular Constructs Using Inkjetting ASME J. of Manufacturing Sci. and Eng. 2014, 136, 061020.

(63) Kloxin, A.M.; Kasko, A.M.; Salinas, C.N.; Anseth, K.S. Photodegradable Hydrogels for Dynamic Tuning of Physical and Chemical Properties Science 2009, 324, 59-63.

Table of Contents Graph